



A new spectral method using Mittag-Leffler wavelets for solving stochastic differential equations

Fateme Yari, Farshid Mirzaee*, and Erfan Solhi

Department of Mathematics, Faculty of Mathematical Sciences and Statistics, Malayer University, Malayer, Iran.

Abstract

This paper introduces a novel numerical method for solving stochastic differential equations using a newly developed basis of Mittag-Leffler wavelets. The proposed approach integrates the collocation and numerical integration methods to approximate solutions, effectively transforming the problem into a nonlinear system of equations that is efficiently solved using the Newton method. The Mittag-Leffler wavelets significantly enhance the effectiveness of the numerical approximations. Numerical experiments, including comparisons with other existing methods, demonstrate the superior accuracy and computational efficiency of the proposed method, especially for nonlinear problems influenced by stochastic noise. The simplicity and robustness of this method make it a powerful tool for solving stochastic problems. These findings underscore the potential of the proposed technique to advance the numerical solution of stochastic differential equations.

Keywords. Mittag-Leffler wavelets, Stochastic differential equations, Collocation method, Numerical integration.

2010 Mathematics Subject Classification. 60H35, 41A58, 65C30, 42C40, 60J65.

1. INTRODUCTION

A stochastic process, also known as a random process, is a mathematical construct that models the evolution of a random phenomenon over time. These processes are characterized by inherent randomness, leading to unpredictable changes as time progresses. Stochastic models are crucial in accurately representing natural phenomena, as they incorporate the random elements inherent in such systems. The inclusion of these stochastic components in mathematical models introduces complexities that hinder the derivation of exact or numerical solutions. From a mathematical standpoint, addressing these complexities has spurred the development of various numerical methods. Stochastic differential equations (SDEs), which frequently emerge across diverse scientific and engineering fields, are of particular significance. Stochastic differential equations arise in a wide range of real-world applications, including financial modeling, where they describe asset prices and interest rate dynamics, and in biological systems, where they capture population growth and neural processes under random perturbations. Highlighting these domains emphasizes the practical significance of the proposed method and mirrors the applied focus of recent studies in the field. Consequently, the study of these models and the advancement of numerical techniques for their resolution are vital areas of research. In recent years, innovative approximation methods have been introduced to obtain numerical solutions to stochastic differential equations, often considering standard Brownian motion. Additionally, the limitations of deterministic models have been identified, further underscoring the importance of stochastic approaches. Notable numerical methods in this domain include the Euler-Maruyama method [7], the Milstein method [22], Runge-Kutta methods [4], Collocation methods [24], and other advanced techniques such as those based on Bernoulli polynomials [25], Hat functions [14], B-spline wavelets [6], and Chebyshev cardinal wavelets [10]. The canonical representation of a stochastic differential equation

Received: 17 March 2025 ; Accepted: 19 October 2025.

* Corresponding author. Email: f.mirzaee@malayeru.ac.ir.

driven by a standard Wiener process, $W(t)$, is expressed as:

$$\begin{cases} d\Phi(\zeta) = \Lambda_1\tau_1(\zeta, \Phi(\zeta))d\zeta + \Lambda_2\tau_2(\zeta, \Phi(\zeta))dW(\zeta), & 0 \leq \zeta \leq \mathfrak{T}, \\ \Phi(0) = \Phi_0, \end{cases} \quad (1.1)$$

where $\Phi(\zeta)$ represents the stochastic process under consideration. Solving such equations analytically is often challenging due to their inherent complexity and the stochastic components involved.

Wavelets are mathematical functions that can decompose complex signals into components at various scales, providing a multi-resolution analysis that is particularly effective for handling localized irregularities and singularities in data. Unlike traditional Fourier analysis, which analyzes signals solely in the frequency domain, wavelets offer a simultaneous time-frequency analysis, allowing for the extraction of more precise information from abrupt, localized signal changes [3]. The application of wavelets to SDEs is recognized as an innovative and efficient approach, especially valuable in analyzing complex systems that involve noise or uncertainty. Wavelets have several applications in approximation theory, particularly in the construction of orthogonal functions. This facilitates the establishment of an orthogonal basis for $\mathcal{L}^2[0, 1]$, enabling efficient representation and analysis of functions within this space. This orthogonality property is crucial for ensuring the stability and convergence of numerical methods. In recent years, various types of polynomial-based wavelets, including Legendre, Laguerre, Bernstein, Euler, Jacobi, and Fibonacci, have been designed and implemented. These wavelets have been utilized to approximate solutions to SDEs, offering advantages such as data compression, multi-scale analysis, and the provision of effective numerical solutions.

In recent years, significant attention has been devoted to the stability and convergence analysis of numerical methods for stochastic differential equations, as these properties are essential to ensure the reliability of computational results. Various stepwise schemes, including Runge–Kutta type and Milstein-type methods, have been developed and rigorously analyzed in this context. For example, the exponential mean-square stability of numerical solutions for stochastic delay integro-differential equations with Poisson jumps has been established [1], and the mean-square stability of diagonally drift Runge–Kutta methods of strong convergence order 1.5 has also been investigated [19]. More recently, stability and convergence properties of stochastic Runge–Kutta and balanced stochastic Runge–Kutta methods have been studied in detail [15]. These works collectively provide a valuable framework for understanding the performance of stochastic numerical methods and offer a useful context for the development of the present wavelet-based spectral approach. In addition to these works, it is also relevant to mention the split-step θ -Milstein method, which has been analyzed for stochastic differential equations with delay terms [2]. This method represents a robust stepwise approach with proven stability properties under appropriate step-size conditions. By contrast, the proposed spectral method based on Mittag–Leffler wavelets provides a fundamentally different perspective. Instead of discretizing the system through stepwise stochastic integrators, our approach constructs global approximations by employing wavelet bases with excellent localization and approximation properties. This transformation reduces the stochastic problem to a system of nonlinear algebraic equations that can be solved efficiently using Newton’s method. Numerical experiments confirm that the wavelet-based approach achieves higher accuracy and greater flexibility compared to step-based schemes, while still maintaining computational efficiency. Situating the proposed method alongside the split-step θ -Milstein approach highlights their methodological differences and clarifies the distinct advantages of each method.

In this paper, we introduce a novel set of basis functions, termed the Mittag-Leffler wavelets, to achieve approximate solutions for stochastic differential equations. By employing these wavelets, we transform the stochastic differential equations into a system of algebraic equations, facilitating efficient numerical solutions. In handling the stochastic noise, the present method employs the Itô approximation for integrals involving random terms. This converts stochastic integrals into summations, which allows for efficient numerical implementation. The examples presented demonstrate that this approach is straightforward and, using a minimal number of points, provides highly accurate results. This efficiency is particularly advantageous in applications where computational resources are limited or where rapid solutions are required. The integration of Mittag-Leffler wavelets into the numerical solution of stochastic differential equations represents a robust framework for addressing the challenges posed by stochastic systems. The flexibility and efficiency of this approach make it a valuable tool for researchers and practitioners dealing with complex stochastic models across various scientific and engineering disciplines.



2. MITTAG-LEFFLER POLYNOMIALS AND WAVELETS

This section is divided into two subsections: the first introduces the Mittag-Leffler polynomials, and the second presents the Mittag-Leffler wavelets.

2.1. Mittag-Leffler Polynomials. In this section, we analyze the Mittag-Leffler polynomials as a class of special polynomials defined by the following generating function:

$$\Gamma(\mathfrak{P}, \zeta) = (1 + \mathfrak{P})^\zeta(1 - \mathfrak{P})^{-\zeta} = \exp\left(\zeta \log\left(\frac{1 + \mathfrak{P}}{1 - \mathfrak{P}}\right)\right) = \sum_{\varkappa=0}^{\infty} \mathfrak{ML}_{\varkappa}(\zeta) \frac{\mathfrak{P}^{\varkappa}}{\varkappa!}. \tag{2.1}$$

The Mittag-Leffler polynomials $\mathfrak{ML}_{\varkappa}(\zeta)$ were introduced in [18]. These polynomials are studied in the context of differential equations and provide an analytical representation of certain integral transforms. The mapping from the ζ -plane to the ϖ -plane is given by the transformation:

$$\varpi = \varpi_0 \left(\frac{1 + \zeta}{1 - \zeta}\right)^F, \tag{2.2}$$

where the parameter F is defined as $\frac{2d}{i\pi}$. The parameter d represents a scaling factor that often appears in conformal mappings and special function theory.

The Mittag-Leffler polynomials are explicitly given by:

$$\mathfrak{ML}_{\eta}(\zeta) = \sum_{i=0}^{\eta} \binom{\eta}{i} (\eta - i)_{\eta-i} 2^i (\zeta)_i, \tag{2.3}$$

where $(\zeta)_i$ denotes the descending factorial, which is defined as $(\zeta)_i = \zeta(\zeta - 1)(\zeta - 2) \cdots (\zeta - (i - 1))$. It is commonly used in combinatorial mathematics and series expansions.

Another polynomial sequence, $\varrho_{\eta}(\zeta)$, is given by:

$$\varrho_{\eta}(\zeta) = \sum_{j=0}^{\eta} \mathbb{S}(\eta; j) \zeta^j = \sum_{j=0}^{\eta} \left\{ \begin{matrix} \eta \\ j \end{matrix} \right\} \zeta^j, \tag{2.4}$$

where $\mathbb{S}(\eta; j)$ represents the Stirling number of the second kind. The Stirling number $\left\{ \begin{matrix} \eta \\ j \end{matrix} \right\}$ counts the number of ways to partition a set of η elements into j non-empty subsets.

Remark 2.1. Based on Vieta’s formulas [8], the following identity is obtained for the descending factorial $(\zeta^t)_{\varkappa}$:

$$\begin{aligned} (\zeta^t)_{\varkappa} &= \zeta^t(\zeta^t - 1) \cdots (\zeta^t - (\varkappa - 1)) \\ &= \zeta^{t\varkappa} - \left(\sum_{j=0}^{\varkappa-1} j\right) \zeta^{t(\varkappa-1)} + \left(\sum_{0 \leq j < i \leq \varkappa-1} ji\right) \zeta^{t(\varkappa-2)} + \cdots + (-1)^{\varkappa} \prod_{j=0}^{\varkappa-1} j \\ &= \sum_{\tau=0}^{\varkappa-1} \mathbb{A}_{\tau} \zeta^{t\tau}. \end{aligned} \tag{2.5}$$

2.2. Mittag-Leffler wavelets. The subsequent relation characterizes a new family of wavelet functions, termed Mittag-Leffler wavelets, on the interval $[0, 1)$. Utilizing Equation (2.3), we conclude:

$$\varphi_{\varkappa, \eta}(\zeta) = \begin{cases} 2^{\frac{\tau-1}{2}} \mathbb{ML}_{\eta}(2^{\tau-1}\zeta + 1 - \varkappa), & \zeta \in \left[\frac{\varkappa-1}{2^{\tau-1}}, \frac{\varkappa}{2^{\tau-1}}\right), \\ 0, & \text{Otherwise,} \end{cases} \tag{2.6}$$

where the function $\mathbb{ML}_{\eta}(2^{\tau-1}\zeta + 1 - \varkappa)$ is given by:

$$\mathbb{ML}_{\eta}(2^{\tau-1}\zeta + 1 - \varkappa) = \frac{1}{\sqrt{\int_0^1 \mathfrak{ML}_{\eta}^2(\zeta) d\zeta}} \times \mathfrak{ML}_{\eta}(2^{\tau-1}\zeta + 1 - \varkappa). \tag{2.7}$$



Here, $\varkappa = 1, 2, \dots, 2^{\mathfrak{T}-1}$, and \mathfrak{T} is a positive integer. The variable ζ represents the normalized time, while $\eta = 0, 1, 2, \dots, \mathfrak{M} - 1$ determines the polynomial degree of the Mittag-Leffler wavelets $\mathfrak{ML}(\zeta)$, as described in equation (2.7) [18].

For the specific case of $\mathfrak{T} = 2$ and $\mathfrak{M} = 3$, the Mittag-Leffler wavelets take the following forms:

$$\begin{aligned}\varphi_{1,0}(\zeta) &= \begin{cases} \sqrt{2}, & 0 \leq \zeta < \frac{1}{2}, \\ 0, & \frac{1}{2} \leq \zeta < 1, \end{cases} \\ \varphi_{2,0}(\zeta) &= \begin{cases} 0, & 0 \leq \zeta < \frac{1}{2}, \\ \sqrt{2}, & \frac{1}{2} \leq \zeta < 1, \end{cases} \\ \varphi_{1,1}(\zeta) &= \begin{cases} 2\sqrt{6}\zeta, & 0 \leq \zeta < \frac{1}{2}, \\ 0, & \frac{1}{2} \leq \zeta < 1, \end{cases} \\ \varphi_{2,1}(\zeta) &= \begin{cases} 0, & 0 \leq \zeta < \frac{1}{2}, \\ \sqrt{6}(2\zeta - 1), & \frac{1}{2} \leq \zeta < 1, \end{cases} \\ \varphi_{1,2}(\zeta) &= \begin{cases} 4\sqrt{10}\zeta^2, & 0 \leq \zeta < \frac{1}{2}, \\ 0, & \frac{1}{2} \leq \zeta < 1, \end{cases} \\ \varphi_{2,2}(\zeta) &= \begin{cases} 0, & 0 \leq \zeta < \frac{1}{2}, \\ \sqrt{10}(2\zeta - 1)^2, & \frac{1}{2} \leq \zeta < 1. \end{cases}\end{aligned}$$

Consequently, the wavelets can be represented as a vector:

$$\Psi(\zeta) = [\varphi_{1,0}(\zeta), \dots, \varphi_{1,\mathfrak{M}-1}(\zeta), \dots, \varphi_{2^{\mathfrak{T}-1},0}(\zeta), \dots, \varphi_{2^{\mathfrak{T}-1},\mathfrak{M}-1}(\zeta)]^T, \quad (2.8)$$

where $\Psi(\zeta)$ is a $2^{\mathfrak{T}-1}\mathfrak{M} \times 1$ vector.

3. STOCHASTIC CALCULUS

In this section, several fundamental definitions related to stochastic calculus are presented.

Definition 3.1. (*Brownian motion*) [12] A real-valued stochastic process $W(\zeta)$, where $\zeta \in [0, \mathfrak{T}]$, is called a Brownian motion if it satisfies the following properties:

- (1) The process has independent increments for $0 \leq \zeta_1 \leq \zeta_2 \leq \dots \leq \zeta_n \leq \mathfrak{T}$.
- (2) For all $\zeta \geq 0$, the increment $W(\zeta + h) - W(\zeta)$ follows a normal distribution with mean zero and variance h .
- (3) The function $\zeta \mapsto W(\zeta)$ is continuous.

Definition 3.2. The Itô integral is defined as

$$I(Z)(\omega) = \int_v^\vartheta Z(\varepsilon, \gamma) dW(\varepsilon)(\omega),$$

in a given space $\Pi = \Pi(v, \vartheta)$ where $0 \leq v \leq \vartheta$. This space consists of functions $Z(\varepsilon, \gamma) : [0, 1] \times \Omega \rightarrow \mathbb{R}^n$ that satisfy the following conditions:

- (1) The function $Z(\varepsilon, \gamma)$ is $\beta \times F$ -measurable, where β is the Borel algebra.
- (2) The function $Z(\varepsilon, \gamma)$ is adapted to the filtration F_ε .
- (3) The expectation satisfies $\mathbb{E} \left[\int_v^\vartheta Z^2(\varepsilon, \gamma) d\varepsilon \right] < \infty$.



The Itô integral of $Z(\varepsilon, \gamma) \in \Pi(v, \vartheta)$ is given by

$$\int_v^\vartheta Z(\varepsilon, \gamma) dW(\varepsilon)(\omega) = \lim_{n \rightarrow \infty} \int_v^\vartheta \Omega_n(\varepsilon, \gamma) dW(\varepsilon)(\omega), \tag{3.1}$$

where Ω_n is a sequence of basic functions satisfying

$$\mathbb{E} \left[\int_v^\vartheta (Z - \Omega_n)^2 d\varepsilon \right] \rightarrow 0, \quad n \rightarrow \infty. \tag{3.2}$$

Lemma 3.3. (Itô Isometry) [21] Suppose $\wp \in \Pi(v, \vartheta)$ is a basic and bounded function on the interval $[0, \zeta]$. Then, the following holds:

$$\mathbb{E} \left[\left(\int_0^\zeta \wp(v, \vartheta) dW(v)(\vartheta) \right)^2 \right] = \mathbb{E} \left[\int_0^\zeta \wp^2(v, \vartheta) dv \right].$$

Proposition 3.4. (Itô Approximation) [11] Let \wp be a measurable stochastic process. The Itô integral $\int_0^\mathfrak{I} \wp(v) dW(v)$ can be approximated using the following relation:

$$\int_0^\mathfrak{I} \wp(v) dW(v) \simeq \sum_{i=1}^{\mathbb{O}} \wp(v_{i-1}) (W(v_i) - W(v_{i-1})).$$

In this formula, \mathbb{O} is an integer, and the partition points are given by

$$v_i = \frac{\mathfrak{I}}{\mathbb{O}} i, \quad i = 1, \dots, \mathbb{O}.$$

4. NUMERICAL SCHEME

This section presents an efficient and straightforward method for solving stochastic differential equations using Mittag-Leffler wavelets. The approach combines a local numerical method with an integral numerical technique. To proceed, the stochastic differential equation given in equation (1.1) must first be transformed into its equivalent stochastic integral form. In handling the stochastic noise, the method employs the Itô approximation for integrals involving random terms. This procedure converts stochastic integrals into summations, which allows for efficient numerical implementation. The validity of this approach is supported by established theoretical results showing that the Itô approximation converges in the mean-square sense to the true solution of the stochastic integral, thereby ensuring the reliability of the proposed wavelet-based scheme. By integrating both sides of the equation, we obtain the following stochastic Itô-Volterra integral equation:

$$\Phi(\zeta) = \theta(\zeta) + \Lambda_1 \int_0^\zeta \tau_1(\chi, \Phi(\chi)) d\chi + \Lambda_2 \int_0^\zeta \tau_2(\chi, \Phi(\chi)) dW(\chi), \quad \zeta \in \mathfrak{D} = [0, \mathfrak{I}], \tag{4.1}$$

where the functions $\tau_1(\chi, \Phi(\chi))$ and $\tau_2(\chi, \Phi(\chi))$ are defined on $\mathfrak{D} \times \mathfrak{D}$, and $\theta(\zeta)$ is defined on \mathfrak{D} . These functions represent stochastic processes defined within a common probability space (Ω, F, P) . Consequently, $\Phi(\zeta)$ denotes the unknown stochastic process, while $W(\chi)$ represents standard Brownian motion. The objective is to determine the unknown function $\Phi(\zeta)$.

For simplicity, let $\mathfrak{I} = 1$. To approximate the unknown function in Equation (4.1), we employ Mittag-Leffler wavelets as basis functions and substitute this approximation into Equation (4.1). The function $\Phi(\zeta)$ is approximated as:

$$\bar{\Phi}_N(\zeta) = \sum_{i=1}^N \Psi_i(\zeta) \mathcal{A}_i,$$



where $\aleph = 2^{\top-1}\mathfrak{M}$. By substituting this approximation into Equation (4.1), we obtain:

$$\sum_{i=1}^{\aleph} \Psi_i(\zeta) \mathcal{A}_i = \theta(\zeta) + \Lambda_1 \int_0^{\zeta} \tau_1(\chi, \sum_{i=1}^{\aleph} \Psi_i(\chi) \mathcal{A}_i) d\chi + \Lambda_2 \int_0^{\zeta} \tau_2(\chi, \sum_{i=1}^{\aleph} \Psi_i(\chi) \mathcal{A}_i) dW(\chi) + \mathcal{R}_{\aleph}(\zeta), \quad (4.2)$$

where $\mathcal{R}_{\aleph}(\zeta)$ represents the residual error resulting from the approximation in Equation (4.2), and $\chi \in [0, \zeta]$.

Next, we consider the deterministic part of Equation (4.2) and perform a variable transformation to map the interval $[0, \zeta]$ onto $[0, 1)$. The transformation is defined as:

$$\chi = \delta\zeta, \quad d\chi = \zeta d\delta, \quad \chi \in [0, \zeta], \quad \delta \in [0, 1).$$

Applying this change of variable, we rewrite the equation as:

$$\sum_{i=1}^{\aleph} \Psi_i(\zeta) \mathcal{A}_i - \Lambda_1 \int_0^1 \tau_1(\delta\zeta, \sum_{i=1}^{\aleph} \Psi_i(\delta\zeta) \mathcal{A}_i) \zeta d\delta - \Lambda_2 \int_0^{\zeta} \tau_2(\chi, \sum_{i=1}^{\aleph} \Psi_i(\chi) \mathcal{A}_i) dW(\chi) \simeq \theta(\zeta). \quad (4.3)$$

To solve this problem, it is necessary to compute the unknown coefficients \mathcal{A}_i . For this purpose, we employ the collocation method. The collocation points are chosen as follows, and we assume that Equation (4.3) holds at these points. According to Property (1.1), we define:

$$\zeta_j = \frac{\mathfrak{J}}{\aleph} j, \quad j = 1, 2, \dots, \aleph, \quad (4.4)$$

where the \aleph points ζ_j are selected within the interval $[0, 1)$ such that $0 \leq \zeta_1 \leq \zeta_2 \leq \dots \leq \zeta_{\aleph} < 1$. The distribution of these nodes may be chosen either uniformly or randomly. Consequently, Equation (4.3) transforms into the following form:

$$\sum_{i=1}^{\aleph} \Psi_i(\zeta_j) \mathcal{A}_i - \Lambda_1 \zeta_j \int_0^1 \tau_1(\delta\zeta_j, \sum_{i=1}^{\aleph} \Psi_i(\delta\zeta_j) \mathcal{A}_i) d\delta - \Lambda_2 \int_0^{\zeta_j} \tau_2(\chi, \sum_{i=1}^{\aleph} \Psi_i(\chi) \mathcal{A}_i) dW(\chi) \simeq \theta(\zeta_j). \quad (4.5)$$

Thus, Equation (4.5) can be rewritten as:

$$\begin{aligned} \sum_{i=1}^{\aleph} \Psi_i(\zeta_j) \mathcal{A}_i - \Lambda_1 \zeta_j \sum_{l=1}^N \Theta_l \tau_1(\Upsilon_l \zeta_j, \sum_{i=1}^{\aleph} \Psi_i(\Upsilon_l \zeta_j) \mathcal{A}_i) \\ - \Lambda_2 \sum_{r=1}^{\mathbb{O}} \tau_2(\chi_{r-1}, \sum_{i=1}^{\aleph} \Psi_i(\chi_{r-1}) \mathcal{A}_i) (W(\chi_r) - W(\chi_{r-1})) \simeq \theta(\zeta_j), \quad j = 1, 2, \dots, \aleph. \end{aligned} \quad (4.6)$$

Here, $\{\Upsilon_l\}_{l=1}^N$ and $\{\Theta_l\}_{l=1}^N$ represent the points and weights of the numerical integration, respectively. Additionally, \mathbb{O} is an integer, and $\chi_r = \frac{\zeta_j r}{\mathbb{O}}$, where $r = 1, \dots, \mathbb{O}$. These results are derived by leveraging the relation established in Property 1. As a result, Equation (4.6) forms a system of nonlinear algebraic equations with unknown coefficients \mathcal{A}_i for $i = 1, 2, \dots, \aleph$.

To solve the problem, we employ Newton's method to iteratively approximate the unknown coefficients. In this work, Simpson's method is applied for numerical integration to minimize computational complexity.

5. ERROR ESTIMATION

In this section, we analyze the error of the proposed approach and provide an estimate. The Sobolev norm of order $\sigma \geq 0$ in the range (r, q) , as described in [5], is given by

$$|\mathcal{Y}|_{I^{\sigma}(r,q)} = \sqrt{\sum_{\varsigma=0}^{\sigma} \|\mathcal{Y}^{(\varsigma)}\|_{\mathcal{L}^2(r,q)}^2}, \quad (5.1)$$

where $\mathcal{Y}^{(\varsigma)}$ represents the ς -th order derivative of \mathcal{Y} .



Furthermore, the seminorm is defined as

$$|\mathcal{Y}|_{I^{e,\sigma;\mathfrak{M};\mathfrak{N}}(0,1)} = \sqrt{\sum_{\varsigma=\min\{\sigma,\mathfrak{M}+1\}}^{\sigma} \mathfrak{N}^{2e-2r} \|\mathcal{Y}^{(\varsigma)}\|_{\mathcal{L}^2(0,1)}^2}, \tag{5.2}$$

$$|\mathcal{Y}|_{I^{e,\sigma;\mathfrak{M};\mathfrak{N}}(0,1)} = \mathfrak{N}^{e-\sigma} \|\mathcal{Y}^{(\sigma)}\|_{\mathcal{L}^2(0,1)}, \tag{5.3}$$

where $\mathfrak{M} \geq \sigma - 1$. If $\mathfrak{N} = 1$, the norm $|\cdot|_{I^{e,\sigma;\mathfrak{M};\mathfrak{N}}}$ coincides with $|\cdot|_{I^{\sigma,\mathfrak{M}}}$, as defined in [5].

Remark 5.1. For each $\mathcal{Y} \in I^{\sigma}(0, 1)$, there exists a constant $\mathfrak{C} > 0$ such that

$$\|\mathcal{Y} - \mathfrak{U}_{\mathfrak{M}}\mathcal{Y}\|_{\mathcal{L}^2(0,1)} \leq \frac{\mathfrak{C}}{\mathfrak{M}^{\sigma}} |\mathcal{Y}|_{I^{\sigma,\mathfrak{M}}(0,1)}, \tag{5.4}$$

and for $1 \leq e \leq \sigma$, we have

$$\|\mathcal{Y} - \mathfrak{U}_{\mathfrak{M}}\mathcal{Y}\|_{I^e(0,1)} \leq \frac{\mathfrak{C}}{\mathfrak{M}^{\sigma-2e+\frac{1}{2}}} |\mathcal{Y}|_{I^{\sigma,\mathfrak{M}}(0,1)}. \tag{5.5}$$

In this case, $\mathfrak{U}_{\mathfrak{M}}\mathcal{Y} = \sum_{\Upsilon=0}^{\mathfrak{M}} \mathcal{Y}_{\Upsilon}\mathfrak{M}\mathfrak{L}_{\Upsilon}(\zeta)$ represents the best approximation of \mathcal{Y} outside the space formed by the Mittag-Leffler polynomials on $(0, 1)$. Moreover, the constant \mathfrak{C} is determined by σ .

Theorem 5.2. Let $\mathcal{Q}_{\varkappa} : ((\varkappa - 1)/2^{\Upsilon-1}, \varkappa/2^{\Upsilon-1}) \rightarrow \mathbb{R}$ be a function in $I^{\sigma}((\varkappa - 1)/2^{\Upsilon-1}, \varkappa/2^{\Upsilon-1})$ for $\varkappa = 1, 2, \dots, 2^{\Upsilon-1}$.

Suppose that the function $\mathcal{F}_{\varkappa}\mathcal{Q}_{\varkappa} : (0, 1) \rightarrow \mathbb{R}$ is defined by

$$(\mathcal{F}_{\varkappa}\mathcal{Q}_{\varkappa})(\zeta) = \mathcal{Q}_{\varkappa}\left(\frac{1}{2^{\Upsilon-1}}(\zeta + \varkappa - 1)\right), \quad \forall \zeta \in (0, 1).$$

Then, for $0 \leq r \leq \sigma$, the following relation holds:

$$\|(\mathcal{F}_{\varkappa}\mathcal{Q}_{\varkappa})^{(r)}\|_{\mathcal{L}^2(0,1)} = 2^{(\Upsilon-1)(\frac{1}{2}-r)} \|\mathcal{Q}_{\varkappa}^{(r)}\|_{\mathcal{L}^2(\frac{\varkappa-1}{2^{\Upsilon-1}}, \frac{\varkappa}{2^{\Upsilon-1}})}. \tag{5.6}$$

Proof. For $0 \leq r \leq \sigma$, we apply the variable transformation $\mathfrak{P} = \frac{1}{2^{\Upsilon-1}}(\zeta + \varkappa - 1)$. This yields

$$\begin{aligned} \|(\mathcal{F}_{\varkappa}\mathcal{Q}_{\varkappa})^{(r)}\|_{\mathcal{L}^2(0,1)}^2 &= \int_0^1 |(\mathcal{F}_{\varkappa}\mathcal{Q}_{\varkappa})^{(r)}(\zeta)|^2 d\zeta \\ &= \int_0^1 \left| \mathcal{Q}_{\varkappa}^{(r)}\left(\frac{1}{2^{\Upsilon-1}}(\zeta + \varkappa - 1)\right) \right|^2 d\zeta \\ &= \int_{\frac{\varkappa-1}{2^{\Upsilon-1}}}^{\frac{\varkappa}{2^{\Upsilon-1}}} 2^{(\Upsilon-1)(-2r)} \left| \mathcal{Q}_{\varkappa}^{(r)}(\mathfrak{P}) \right|^2 2^{\Upsilon-1} d\mathfrak{P} \\ &= 2^{(\Upsilon-1)(1-2r)} \|\mathcal{Q}_{\varkappa}^{(r)}\|_{\mathcal{L}^2(\frac{\varkappa-1}{2^{\Upsilon-1}}, \frac{\varkappa}{2^{\Upsilon-1}})}^2. \end{aligned} \tag{5.7}$$

Taking the square root on both sides, we obtain Equation (5.6), completing the proof. □

Theorem 5.3. Let $\mathcal{Y} \in I^{\sigma}(0, 1)$ with $\sigma \geq 0$. Then, the following inequality holds:

$$\|\mathcal{Y} - \mathfrak{U}_{\mathfrak{M}-1}^{2^{\Upsilon-1}}\mathcal{Y}\|_{\mathcal{L}^2(0,1)} \leq \mathfrak{C}(\mathfrak{M} - 1)^{-\sigma} |\mathcal{Y}|_{I^{0;\sigma;\mathfrak{M}-1;2^{\Upsilon-1}}(0,1)}. \tag{5.8}$$

Moreover, for $1 \leq e \leq \sigma$, we obtain:

$$\|\mathcal{Y} - \mathfrak{U}_{\mathfrak{M}-1}^{2^{\Upsilon-1}}\mathcal{Y}\|_{I^e(0,1)} \leq \mathfrak{C}(\mathfrak{M} - 1)^{2e-\sigma-\frac{1}{2}} |\mathcal{Y}|_{I^{e;\sigma;\mathfrak{M}-1;2^{\Upsilon-1}}(0,1)}. \tag{5.9}$$

Proof. The proof follows similarly to the one given in [16]. □



Theorem 5.4. Let $\mathcal{Y} \in I^\sigma(0, 1)$ with $\sigma \geq 0$ and assume that $\mathfrak{M} - 1 \geq \sigma - 1$. Consequently, by applying the previous theorem, it follows that:

$$\left\| \mathcal{Y} - \mathfrak{U}_{\mathfrak{M}-1}^{2^{\mathfrak{T}-1}} \mathcal{Y} \right\|_{\mathcal{L}^2(0,1)} \leq \frac{\mathfrak{e}}{(\mathfrak{M}-1)^\sigma (2^{\mathfrak{T}-1})^\sigma} \left\| \mathcal{Y}^{(\sigma)} \right\|_{\mathcal{L}^2(0,1)}. \quad (5.10)$$

Furthermore, for $e \geq 1$, we have:

$$\left\| \mathcal{Y} - \mathfrak{U}_{\mathfrak{M}-1}^{2^{\mathfrak{T}-1}} \mathcal{Y} \right\|_{I^e(0,1)} \leq \frac{\mathfrak{e}}{(\mathfrak{M}-1)^{\sigma-2e+\frac{1}{2}} (2^{\mathfrak{T}-1})^{\sigma-e}} \left\| \mathcal{Y}^{(\sigma)} \right\|_{\mathcal{L}^2(0,1)}. \quad (5.11)$$

This finding suggests that for an infinitely smooth \mathcal{Y} , the convergence rate of $\mathfrak{U}_{\mathfrak{M}-1}^{2^{\mathfrak{T}-1}} \mathcal{Y}$ to \mathcal{Y} is faster than $(1/2^{\mathfrak{T}-1})$ raised to the power of $(\mathfrak{M} - e)$, as well as any power of $1/(\mathfrak{M} - 1)$. This demonstrates a higher rate of convergence compared to conventional spectral methods [5].

Theorem 5.5. Let $\Phi(\zeta)$ be the exact solution and $\bar{\Phi}_{\mathfrak{N}}(\zeta)$ be the Mittag-Leffler wavelet approximation of the solution to Equation (4.1). Furthermore, suppose the following conditions hold:

1. For every $\mathfrak{T} > 0$, there exists a constant $\mathcal{D} > 0$ such that for all $\eta_1, \eta_2 \in \mathbb{R}$ and $\zeta \in [0, \mathfrak{T}]$,

$$|\tau_1(\zeta, \eta_1) - \tau_1(\zeta, \eta_2)| + |\tau_2(\zeta, \eta_1) - \tau_2(\zeta, \eta_2)| \leq \mathcal{D}|\eta_1 - \eta_2|.$$
2. The coefficients satisfy the linear growth condition:

$$|\tau_1(\zeta, \eta)| + |\tau_2(\zeta, \eta)| \leq \mathcal{D}(1 + |\eta|).$$
3. $\mathbb{E}(|\eta|^2) < \infty$.

Then, $\bar{\Phi}_{\mathfrak{N}}(\zeta)$ converges to $\Phi(\zeta)$ in the \mathcal{L}^p -norm for $1 \leq p \leq q$.

Proof. Define the error term as $e_{\mathfrak{N}}(\zeta) = \Phi(\zeta) - \bar{\Phi}_{\mathfrak{N}}(\zeta)$. Subtracting the equation for $\bar{\Phi}_{\mathfrak{N}}(\zeta)$ from the exact solution, we obtain:

$$e_{\mathfrak{N}}(\zeta) = \Lambda_1 \int_0^\zeta (\tau_1(\chi, \Phi(\chi)) - \tau_1(\chi, \bar{\Phi}_{\mathfrak{N}}(\chi))) d\chi + \Lambda_2 \int_0^\zeta (\tau_2(\chi, \Phi(\chi)) - \tau_2(\chi, \bar{\Phi}_{\mathfrak{N}}(\chi))) dW(\chi).$$

Taking the expectation of $|e_{\mathfrak{N}}(\zeta)|^2$, we write:

$$\mathbb{E}(|e_{\mathfrak{N}}(\zeta)|^2) = \mathbb{E} \left(\left| \Lambda_1 \int_0^\zeta (\tau_1(\chi, \Phi(\chi)) - \tau_1(\chi, \bar{\Phi}_{\mathfrak{N}}(\chi))) d\chi \right|^2 \right) + \mathbb{E} \left(\left| \Lambda_2 \int_0^\zeta (\tau_2(\chi, \Phi(\chi)) - \tau_2(\chi, \bar{\Phi}_{\mathfrak{N}}(\chi))) dW(\chi) \right|^2 \right).$$

Using the Itô isometry for the stochastic integral term, we obtain:

$$\mathbb{E}(|e_{\mathfrak{N}}(\zeta)|^2) \leq \Lambda_1^2 \mathbb{E} \left(\left| \int_0^\zeta (\tau_1(\chi, \Phi(\chi)) - \tau_1(\chi, \bar{\Phi}_{\mathfrak{N}}(\chi))) d\chi \right|^2 \right) + \Lambda_2^2 \zeta \mathbb{E}(|\tau_2(\chi, \Phi(\chi)) - \tau_2(\chi, \bar{\Phi}_{\mathfrak{N}}(\chi))|^2).$$

By applying the Lipschitz continuity of τ_1 and τ_2 , we get:

$$\mathbb{E}(|e_{\mathfrak{N}}(\zeta)|^2) \leq \Lambda_1^2 \mathcal{D}^2 \left(\int_0^\zeta \mathbb{E}(|e_{\mathfrak{N}}(\chi)|) d\chi \right)^2 + \Lambda_2^2 \mathcal{D}^2 \int_0^\zeta \mathbb{E}(|e_{\mathfrak{N}}(\chi)|^2) d\chi.$$

Considering the error term in Simpson's quadrature and defining $\mathfrak{X} = \Lambda_1^2 \mathcal{D}^2 + \Lambda_2^2 \mathcal{D}^2$, we obtain:

$$\mathbb{E}(|e_{\mathfrak{N}}(\zeta)|^2) \leq \mathfrak{X} \int_0^\zeta \mathbb{E}(|e_{\mathfrak{N}}(\chi)|^2) d\chi + \frac{\mathfrak{T} \mathfrak{h}^4}{180} \max_{\chi \in [0, \mathfrak{T}]} |\tau_1^{(4)}(\chi)|.$$

By applying Gronwall's inequality, we obtain:

$$\mathbb{E}(|e_{\mathfrak{N}}(\zeta)|^2) \leq \frac{\mathfrak{T} \mathfrak{h}^4}{180} \max_{\chi \in [0, \mathfrak{T}]} |\tau_1^{(4)}(\chi)| e^{\mathfrak{X} \zeta}.$$

As $\mathfrak{h} \rightarrow 0$, the Simpson's quadrature error tends to zero. Consequently, $\mathbb{E}(|e_{\mathfrak{N}}(\zeta)|^2) \rightarrow 0$ as $\mathfrak{h} \rightarrow 0$. This argument can be extended to the \mathcal{L}^p -norm for $1 \leq p \leq q$. Thus, for sufficiently small \mathfrak{h} , the approximation error vanishes, proving that the Mittag-Leffler wavelet approximation $\bar{\Phi}_{\mathfrak{N}}(\zeta)$ converges to $\Phi(\zeta)$ in \mathcal{L}^p . \square



6. EXAMPLES

In this section, the effectiveness and efficiency of the proposed method are examined through two numerical examples. All numerical computations are performed using MATLAB software. The corresponding numerical results and graphical representations for each example are provided. Due to the presence of randomness in the examples, the numerical outcomes exhibit some variations across different executions. To ensure the validity and reliability of the results, statistical methods are employed, and the final results are presented based on multiple runs. The symbol σ^2 represents the sample variance obtained from the results of the approximate solutions.

Example 6.1. Consider the following stochastic differential equation [12, 13, 23]:

$$d\Phi(\zeta) = -\left(\frac{1}{30}\right)^2 \Phi(\zeta)(1 - \Phi(\zeta)^2)d\zeta + \frac{1}{30}(1 - \Phi(\zeta)^2)dW(\zeta), \quad \zeta \in [0, 1], \tag{6.1}$$

with the initial condition $\Phi(0) = \theta = \frac{1}{10}$.

The exact solution to this equation is given by

$$\Phi(\zeta) = \tanh\left(\frac{1}{30}W(\zeta) + \operatorname{arctanh}(\theta)\right), \tag{6.2}$$

where we take $\theta = \frac{1}{10}$.

The numerical results obtained using the proposed method for different values of \aleph are presented in Tables 1 and 2. Additionally, Figures 1 and 2 illustrate the computed numerical results.

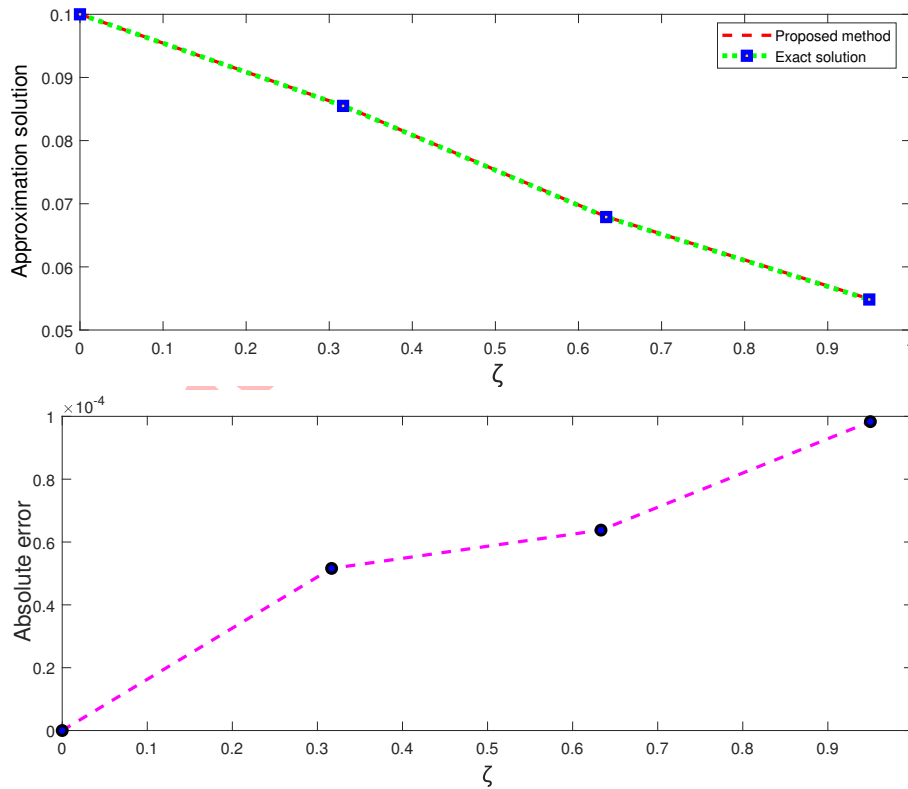
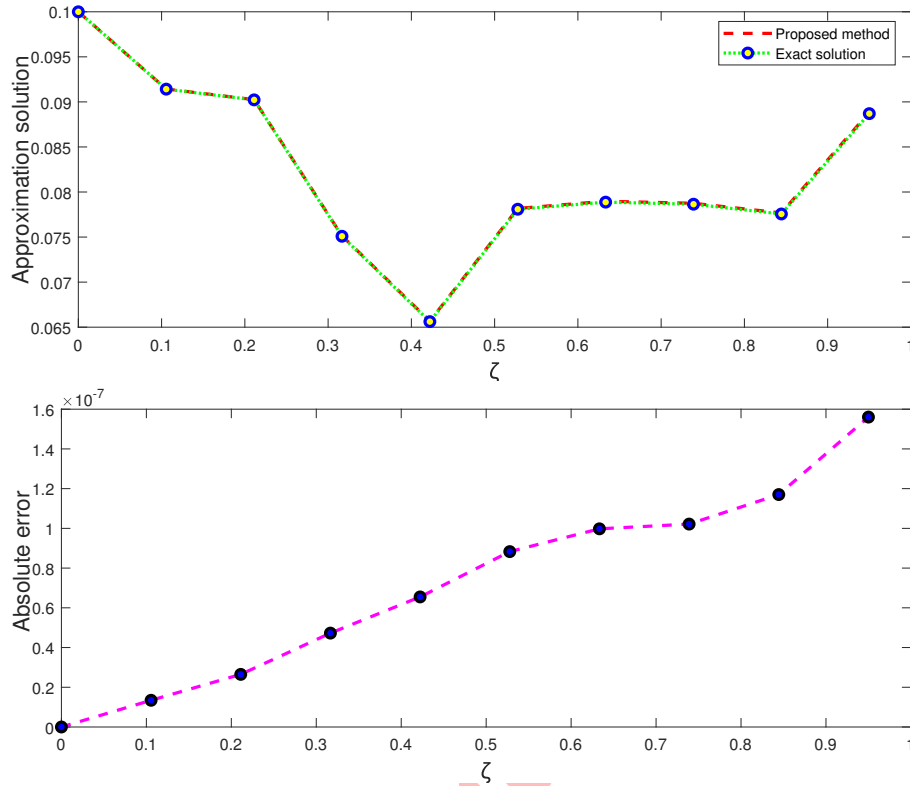


FIGURE 1. Graphs of numerical results of Example 6.1 for $\aleph = 4$.



FIGURE 2. Graphs of numerical results of Example 6.1 for $N = 10$.TABLE 1. Numerical results obtained using the proposed method for $N = 4$, $\mathcal{T} = 2$, and $\mathcal{M} = 2$ for Example 6.1.

ζ	Mean of $\bar{\Phi}_N(\zeta)$	Standard error of mean	σ^2 of sample	0.95 Confidence interval	
				Lower bound	Upper bound
0	0	0	0	0	0
0.32	6.46317E-10	5.7708E-10	6.66043E-18	1.85416E-09	-5.61525E-10
0.63	5.08685E-09	4.12373E-09	3.40103E-16	1.37179E-08	-3.54422E-09
0.95	2.12009E-08	1.21258E-08	2.94072E-15	4.65806E-08	-4.17877E-09

Example 6.2. Consider the following stochastic differential equation [12, 20, 26]:

$$d\Phi(\zeta) = \left(\frac{1}{8}\right)^2 \cos(\Phi(\zeta)) \sin^3(\Phi(\zeta)) d\zeta - \frac{1}{8} \sin^2(\Phi(\zeta)) dW(\zeta), \quad \zeta \in [0, 1), \quad (6.3)$$

with the initial condition $\Phi(0) = \theta = \frac{\pi}{32}$.

The exact solution to this equation is given by

$$\Phi(\zeta) = \arccot \left(\frac{1}{8} W(\zeta) + \cot(\zeta) \right). \quad (6.4)$$

The numerical results obtained using the proposed method for different values of N are presented in Tables 3 and 4. Additionally, Figures 3 and 4 illustrate the computed numerical results.



TABLE 2. Numerical results obtained using the proposed method for $\aleph = 10$, $\beth = 2$, and $\mathfrak{M} = 5$ for Example 6.1.

ζ	Mean of $\bar{\Phi}_{\aleph}(\zeta)$	Standard error of mean	σ^2 of sample	0.95 Confidence interval	
				Lower bound	Upper bound
0	0	0	0	0	0
0.105	1.58232E-11	1.6105E-11	5.18739E-21	4.95312E-11	-1.78849E-11
0.211	2.7762E-09	2.74888E-09	1.51126E-16	8.52973E-09	-2.97719E-09
0.316	2.5396E-09	2.51016E-09	1.26018E-16	7.7934E-09	-2.71422E-09
0.422	3.04646E-09	2.73724E-09	1.4985E-16	8.77554E-09	-2.68267E-09
0.527	1.52756E-09	1.47322E-09	4.34074E-17	4.81104E-09	-1.55591E-09
0.633	2.72437E-10	2.31804E-10	1.7466E-18	7.57608E-10	-2.12735E-10
0.738	8.37497E-10	1.28794E-09	3.31758E-17	3.53319E-09	-1.85819E-09
0.844	1.70277E-09	1.13201E-09	2.56288E-17	4.07209E-09	-6.66544E-10
0.950	-1.79753E-09	2.0031E-09	8.02483E-17	2.395E-09	-5.99007E-09

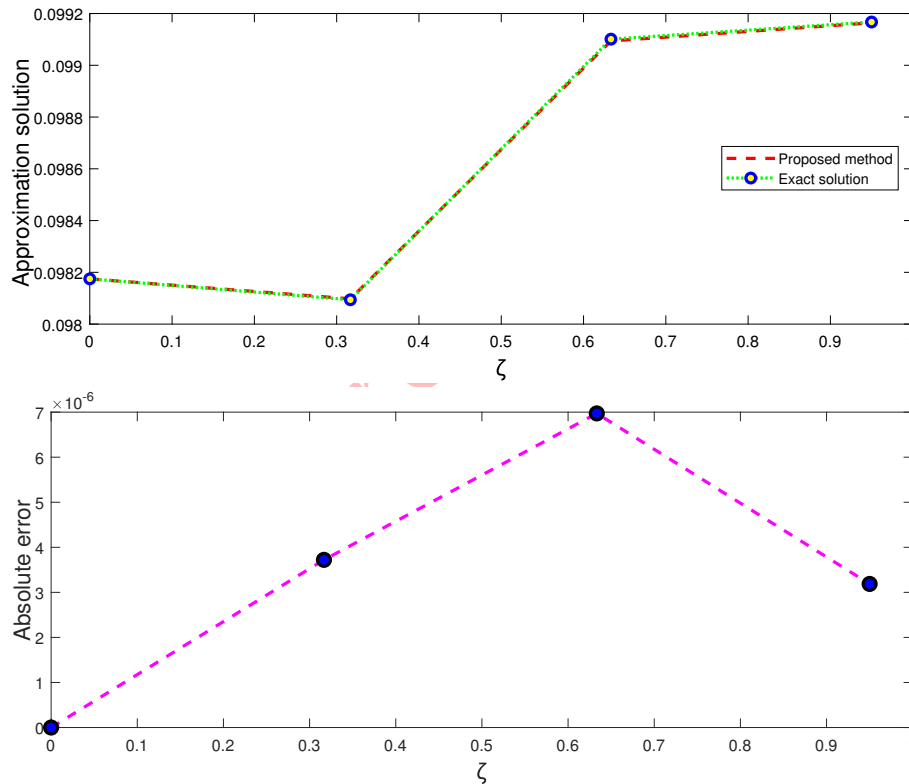
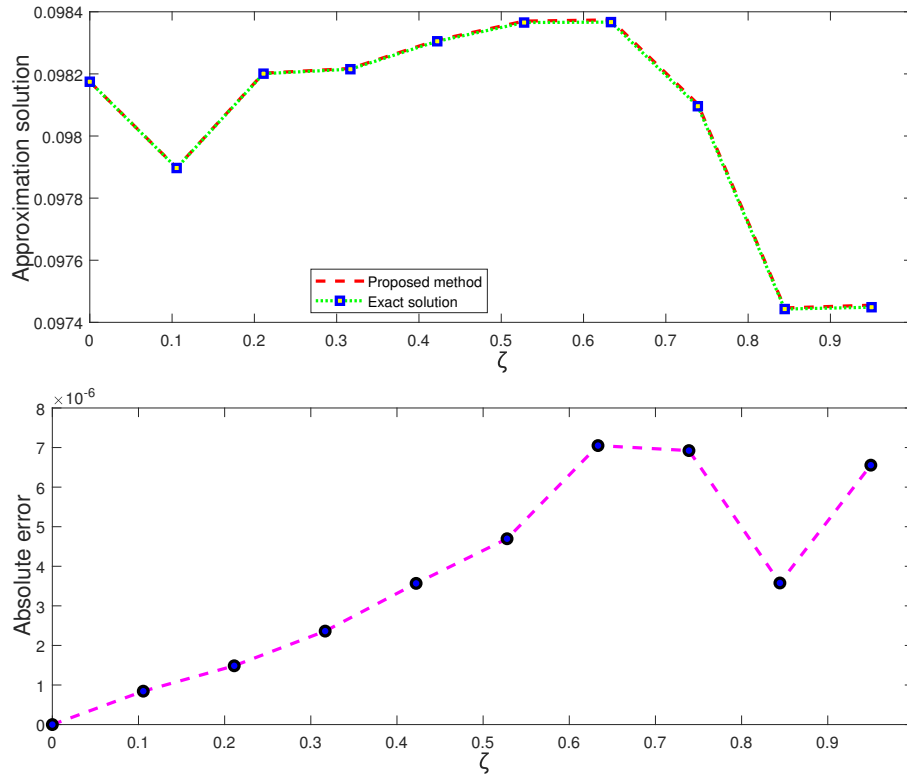


FIGURE 3. Graphs of numerical results of Example 6.2 for $\aleph = 4$.

7. CONCLUSION

In this article, we have introduced a novel approach for solving stochastic differential equations by transforming them into stochastic integral equations. We have introduced the Mittag–Leffler wavelets as a novel set of basis functions for approximating the unknown functions in these equations. By employing numerical integration and collocation methods,



FIGURE 4. Graphs of numerical results of Example 6.2 for $N = 10$.TABLE 3. Numerical results obtained using the proposed method for $N = 4$, $\mathcal{T} = 2$, and $\mathcal{M} = 2$ for Example 6.2.

ζ	Mean of $\bar{\Phi}_N(\zeta)$	Standard error of mean	σ^2 of sample	0.95 Confidence interval	
				Lower bound	Upper bound
0	1.38777E-18	3.16784E-18	2.00704E-34	8.01813E-18	-5.24259E-18
0.32	2.25134E-09	7.51682E-09	1.13005E-15	1.79842E-08	-1.34815E-08
0.63	5.1862E-09	1.9131E-08	7.3199E-15	4.52278E-08	-3.48554E-08
0.95	1.35454E-09	1.69716E-08	5.7607E-15	4.90673E-08	-2.19765E-08

we have converted the problem into a system of equations that can be efficiently solved. In addition, to handle the stochastic noise, the method applies the Itô approximation to integrals involving random terms. This converts the stochastic integrals into summations, enabling practical implementation. The numerical results obtained from the examples demonstrate that our method is simpler than existing methods and provides higher accuracy with fewer computational resources. This efficiency is particularly advantageous in applications where computational resources are limited or where rapid solutions are required. The application of Mittag-Leffler wavelets into the numerical solution of stochastic differential equations represents a robust framework for addressing the challenges posed by stochastic systems. The flexibility and efficiency of this approach make it a valuable tool for researchers and practitioners dealing with complex stochastic models across various scientific and engineering disciplines.



TABLE 4. Numerical results obtained using the proposed method for $\aleph = 10$, $\daleth = 2$, and $\mathfrak{M} = 5$ for Example 6.2.

ζ	Mean of $\bar{\Phi}_{\aleph}(\zeta)$	Standard error of mean	σ^2 of sample	0.95 Confidence interval	
				Lower bound	Upper bound
0	-2.08165E-18	3.06622E-18	1.88034E-34	4.33603E-18	-8.49933E-18
0.105	7.33639E-09	4.03519E-09	3.25655E-16	1.57821E-08	-1.10935E-09
0.211	1.1607E-08	6.16219E-09	7.59451E-16	2.45046E-08	-1.29065E-09
0.316	1.91056E-08	7.78475E-09	1.21205E-15	3.53993E-08	2.81196E-09
0.422	1.52463E-08	9.26072E-09	1.71522E-15	3.46292E-08	-4.13663E-09
0.527	2.1258E-08	1.46945E-08	4.31855E-15	5.20138E-08	-9.49791E-09
0.633	1.80966E-08	1.17849E-08	2.77767E-15	4.27626E-08	-6.56948E-09
0.738	-1.64695E-08	1.57514E-08	4.96216E-15	1.64986E-08	-4.94377E-08
0.844	1.67539E-08	1.20293E-08	2.89409E-15	4.19316E-08	-8.42374E-09
0.950	2.8152E-08	2.20547E-08	9.72823E-15	7.43131E-08	-1.80091E-08

ETHICAL APPROVAL

This article does not contain any studies with human participants performed by any of the authors.

AVAILABILITY OF SUPPORTING DATA

No data were used to support the findings of the study.

CONFLICT OF INTEREST

The authors declare that they have no known competing financial interests or personal relationships that could have appeared to influence the work reported in this paper, subject matter or materials discussed in this manuscript.

FUNDING

This research received no specific grant from any funding agency in the public, commercial, or not-for-profit sectors.

ACKNOWLEDGEMENTS

The authors would like to express our appreciation to the editor and referees for their valuable comments and constructive suggestions, which have enhanced the quality of this paper.

REFERENCES

- [1] D. Ahmadian and O. Farkhondeh Rouz, *Exponential mean-square stability of numerical solutions for stochastic delay integro-differential equations with Poisson jump*, Journal of Inequalities and Applications, 186(2020) (2020), 1–33.
- [2] D. Ahmadian and O. Farkhondeh Rouz, *Stability analysis of split-step θ -Milstein method for a class of n -dimensional stochastic differential equations*, Applied Mathematics and Computation, 348 (2019), 201–215.
- [3] N. Alam Khan, M. Ali, A. Ara, M. Ijaz Khan, S. Abdullaeva, and M. Waqas, *Optimizing pantograph fractional differential: A Haar wavelet operational matrix method*, Partial Differential Equations Applied Mathematics, 11 (2024), 100774.
- [4] R. Ambrosio and C. Scalone, *Two-step Runge-Kutta methods for stochastic differential equations*, Applied Mathematics and Computing, 403 (2021), 125930.
- [5] C. Canuto, M. Hussaini, A. Youssuff Quarteroni, and T. A. Zang, *Spectral Methods: Fundamentals in Single Domains*, Berlin: Springer, (2006).



- [6] A. Elahi, S. Irandoust-pakchin, A. Rahimi, and S. Abdi-mazraeh, *A new approach of B-spline wavelets to solve fractional differential equations*, Communications in Nonlinear Science and Numerical Simulation, 136 (2024), 108099.
- [7] H. R. Erfanian, M. Hajimohammadi, and M. J. Abdi, *Using the Euler-Maruyama method for finding a solution to stochastic financial problems*, International Journal of Intelligent Systems and Applications, 8(6) (2016), 48–55.
- [8] H. G. Funkhouser, *A short account of the history of symmetric functions of roots of equations*, The American Mathematical Monthly, 37(7) (1930), 357–365.
- [9] A. Ghasempour, Y. Ordokhani, and S. Sabermahani, *Mittag-Leffler wavelets and their applications for solving fractional optimal control problems*, Journal of Vibration and Control, 3(5-6) (2024), 1–15.
- [10] M. H. Heydari, M. R. Mahmoudi, A. Shakiba, and Z. Avazzadeh, *Chebyshev cardinal wavelets and their application in solving nonlinear stochastic differential equations with fractional Brownian motion*, Communications in Nonlinear Science and Numerical Simulation, 64 (2018), 98–121.
- [11] D. J. Higham, *An algorithmic introduction to numerical simulation of stochastic differential equations*, SIAM Review, 43(3) (2001), 525–546.
- [12] F. Mirzaee, S. Naserifar, and E. Solhi, *Accurate and stable numerical based on the Floater-Hormann interpolation for stochastic Itô-Volterra integral equations*, Numerical Algorithms, 94(1) (2023), 275–292.
- [13] F. Mirzaee, E. Solhi, and N. Samadyar, *Moving least squares and spectral collocation method to approximate the solution of stochastic Volterra-Fredholm integral equations*, Applied Numerical Mathematics, 161 (2021), 275–285.
- [14] J. K. Mohammed and A. R. Khudair, *Solving nonlinear stochastic differential equations via fourth-degree hat functions*, Results in Control and Optimization, 12(1) (2023), 100291.
- [15] V. Rahimi, D. Ahmadian, and A. Rathinasamy, *Stability and convergence analysis of stochastic Runge-Kutta and balanced stochastic Runge-Kutta methods for solving stochastic differential equations*, Journal of Applied Mathematics and Computing, 71(2) (2025), 1397–1417.
- [16] P. Rahimkhani, Y. Ordokhani, and E. Babolian, *Müntz-Legendre wavelet operational matrix of fractional-order integration and its applications for solving the fractional pantograph differential equations*, Numerical Algorithms, 77(2) (2018), 1283–1305.
- [17] P. E. Ricci and C. V. Emanuele, *Mittag-Leffler polynomial differential equation*, Jnanabha, 48(2) (2018), 1–6.
- [18] S. Roman, *The umbral calculus*, Pure and Applied Mathematics MA: Academic Press Inc., 111 (1984).
- [19] M. Shahmoradi, D. Ahmadian, and M. Ranjbar, *Mean-square stability of 1.5 strong convergence orders of diagonally drift Runge-Kutta methods for a class of stochastic differential equations*, Computational and Applied Mathematics, 40(4) (2021), 108.
- [20] P. Singh and S. Saha Ray, *Two reliable methods for numerical solution of nonlinear stochastic Itô-Volterra integral equation*, Stochastic Analysis and Applications, 40(3) (2021), 1–23.
- [21] E. Solhi, F. Mirzaee, and S. Naserifar, *Approximate solution of two dimensional linear and nonlinear stochastic Itô-Volterra integral equations via meshless scheme*, Mathematics and Computers in Simulation, 207 (2023), 369–387.
- [22] L. Weng and W. Liu, *Invariant measures of the Milstein method for stochastic differential equations with commutative noise*, Applied Mathematics and Computation, 358 (2018), 169–176.
- [23] J. Wu, G. Jiang, and X. Sang, *Advances in Continuous and Discrete Models*, Advances in Difference Equations, 503(2019) (2019), 1–14.
- [24] Y. Xiao, X. Xu, and H. Zhang, *Collocation methods for nonlinear stochastic Volterra integral equations*, Computational and Applied Mathematics, 39(4) (2020), 40.
- [25] R. Zeghdane, *Numerical solution of stochastic integral equations by using Bernoulli operational matrix*, Mathematics and Computers in Simulation, 165 (2019), 238–254.
- [26] R. Zeghdane, *New numerical method for solving nonlinear stochastic integral equations*, Vladikavkazskii Matematicheskii Zhurnal, 22(4) (2020), 68–86.

